

## **INTERPHASE INTEGRITY OF NEUTRON IRRADIATED SILICON CARBIDE COMPOSITES** – L. L. Snead and E. Lara-Curzio (Oak Ridge National Laboratory)

### **OBJECTIVE**

The objective of this study is to apply a residual stress analysis to the interface between Nicalon™ fiber and the interphase coating to explain the experimental result of debonding during neutron irradiation.

### **SUMMARY**

SiC/SiC composites were fabricated from Hi-Nicalon™ fibers with carbon, pseudo-porous SiC and multilayer SiC interphases. These materials were then irradiated in the High Flux Beam Reactor with fast neutrons to a dose level equivalent to 1.1 dpa. Results are presented for bend strength of both non-irradiated and irradiated materials. Degradation in ultimate bend stress was seen for all materials studied, while the matrix micro-cracking stress was unchanged. Within the interphases studied the multilayer SiC interphase material showed the least degradation (8-20%) in ultimate bend stress, while porous SiC underwent the greatest degradation (~35%). The fiber matrix interphases are studied with TEM for both non-irradiated and irradiated materials. While no irradiation induced microstructural evolution of the interphase was observed, debonding of the interphase from the fiber was observed for all cases. This debonding is attributed tensile stresses developed at the interface due to densification of the Hi-Nicalon™ fiber. Residual stress analysis of the fiber matrix interface clearly indicates that for densification of Hi-Nicalon™ and volumetric expansion of the CVD SiC matrix corresponding to these irradiation conditions tensile stresses occur well in excess of those which can be withstood by these, or any other viable SiC composite interphase.

### **PROGRESS AND STATUS**

#### **1. Introduction**

Both the physical and dimensional properties of ceramic grade Nicalon™ fiber are unstable at relatively low neutron fluence [1-3]. The general behavior of these fibers is the inverse of what occurs in fully dense SiC. For example, fully dense SiC undergoes minor isotropic expansion under irradiation while Nicalon™ fiber shows a substantial densification. The elastic modulus and strength of stoichiometric SiC decrease slightly under neutron irradiation while Nicalon™ shows a significant increase. The significant densification of the ceramic grade Nicalon™ (about 5% at 1 displacement per atom, dpa) has been blamed for the substantial (~40%) reduction in bend strength which occurs in CVI SiC matrix composites [4]. The densification of ceramic grade Nicalon™, Hi-Nicalon™ and Morton CVD SiC is given in Figure 1 [5]. Recently, the Nicalon™ fiber thermomechanical properties have been improved by altering the method of cross-linking the spun polymer thereby reducing the oxygen content from 15%. (ceramic grade Nicalon™ fiber) to less than 0.5 % (Hi-Nicalon™) [6]. The average SiC crystallite size for this product increases by more than a factor of two over the ceramic grade fiber, and the fiber elastic modulus undergoes a large increase while the strength decreases slightly. The density of the Hi-Nicalon™ fiber is also increased from 2.55 g/cc (ceramic grade Nicalon™ fiber) to 2.74 g/cc, which is approximately 85 % theoretical SiC density. Also of interest for nuclear applications, the Hi-Nicalon™ fiber density did not undergo the dramatic densification seen in ceramic grade Nicalon™ fiber [5]. Composites produced similarly to those in this study fibers show similar degradation to those fabricated with the ceramic grade Nicalon™, albeit to a lesser extent [5].

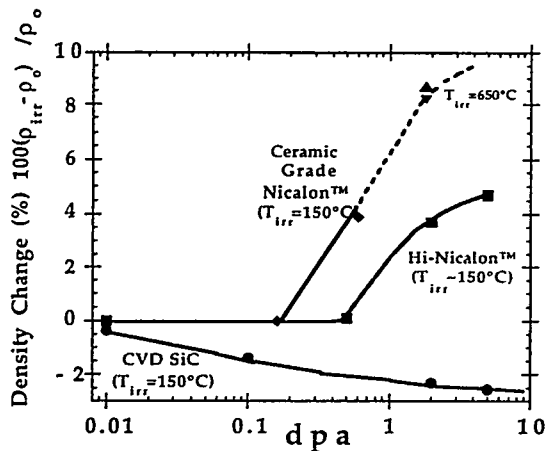


Figure 1: Volumetric changes under irradiation.

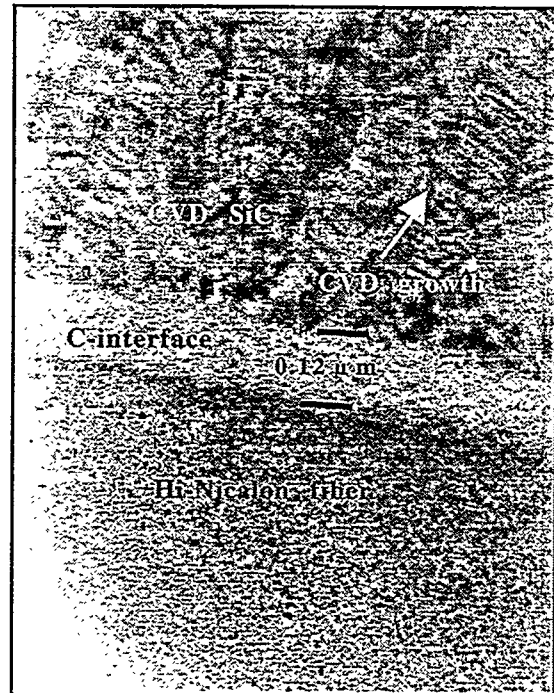


Figure 2: TEM of pyrolytic C interphase.

## 2. EXPERIMENTAL

### Materials

A series of composites were fabricated to deposit a porous SiC interphase first on ceramic grade Nicalon fiber to optimize the process and then on low oxygen content Hi-Nicalon fiber for the irradiation study. The carbon interface was applied to the composite prior to SiC infiltration by decomposition of propylene gas at 1100 °C. Figure 2 shows a TEM micrograph for the 0.12 μm carbon interphase. Previous work has shown that the structure of this interphase deposited onto Nicalon™ in a similar manner is only partially graphitic with basal planes preferentially lying normal to the axis of the fiber [7]. The interface between the Hi-Nicalon™ fiber and the carbon interphase does not show evidence of the silica layer present in ceramic grade Nicalon™ materials processed in a similar fashion. Deposition variables for the porous SiC interphase were infiltration temperature and the relative mixture of methyltrichlorosilane, argon, methane and hydrogen flow gasses. A substantial degradation of the standard Nicalon fiber was seen due to interaction with the (porous SiC) reactant gasses leading to very low composite strengths, especially on the higher temperature surface of the preform, presumably due to accelerated kinetics. For this reason, a thin (0.1 μm) coating of carbon from a propylene precursor was deposited on fibers prior to the porous SiC deposition as a reaction barrier. The results of the process development led to a composite infiltrated at 900°C. Figure 3 shows a high resolution TEM image of the "porous" SiC interphase. This micrograph shows interconnected β-SiC surrounding islands of poorly graphitized carbon. This interphase is best described as a two component mixture of carbon and β-SiC, where the SiC is the predominant phase. The porous and pyrolytic carbon SiC interfacial composites were processed at the High Temperature Materials Laboratory at the Oak Ridge National Laboratory using the forced chemical vapor infiltration (FCVI) method [8]. The infiltrated silicon carbide matrix was deposited from methyltrichlorosilane with a typical infiltration time of 18 hrs. The dimensions of the as fabricated discs were 4.45 cm diameter and 1.25 cm thickness.

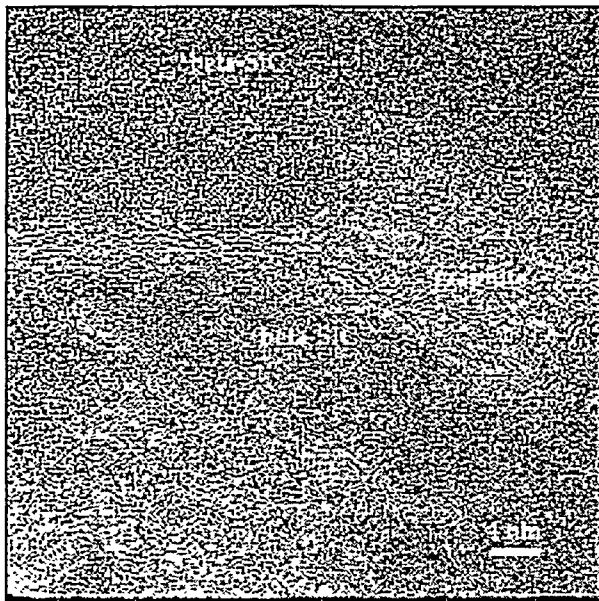


Figure 3: HRTEM of porous SiC interphase.

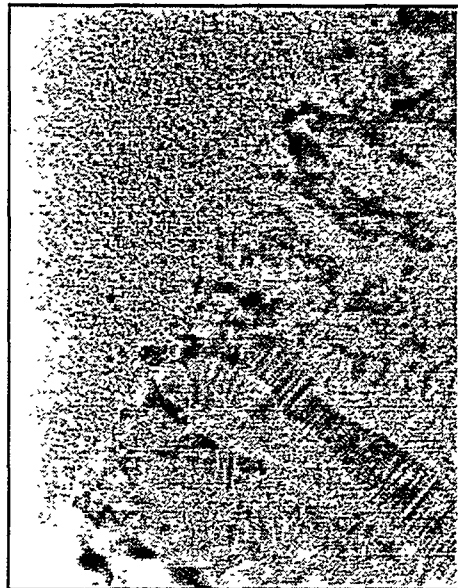


Figure 4: TEM image of interface between fiber and first multilayer SiC interphase.

Composites containing a multilayer SiC fiber coating were fabricated using isothermal CVI of Hi-Nicalon™ fiber preforms by Hyper-Therm High-Temperature Composites, Inc. The fabric was cut into individual plies 15 × 30 cm and laid-up in a (0,90)<sub>s</sub> fiber architecture containing 8 plies per preform. The preform was compacted to ~35% fiber volume within a graphite holding tool during deposition of the fiber coating and subsequent SiC matrix densification. An initial layer of pyrolytic carbon 20 nm thick was deposited on the fiber preform to prevent the previously discussed interaction with the SiC processing phases. The first SiC layer of the multilayer fiber coating is then deposited followed by a 20 nm interrupted layer of pyrolytic carbon. A TEM image of the interface between the fiber and the first interlayer is given in Figure 4. The composite architecture for all composites was 1800 denier (500 filament yarn) plain weave fabric and was laid-up inside a graphite holder with a fiber volume fraction of approximately 40%. The fabricated composite void fraction was 10-12%.

### **Irradiation**

Composite samples were machined to dimensions of 2.5 × 3 × 25 mm for the irradiation study. The porous SiC material surfaces were machined such that the top and bottom surfaces had exposed fabric where the surface layer had been ground flat. The multilayer SiC material had a thin CVD SiC overcoat (~100 μm) so that the top and bottom fabric layer were not exposed. The fabric orientation was such that the fabric was in the plane of the width and length axes of the bend bar. All edges of the bend bars were ground flat, thus some of the fibers were machined away for the porous SiC interfacial materials. All materials were cleaned in acetone and isopropyl alcohol prior to the irradiation capsule assembly.

A single irradiation capsule, SiC-1, was assembled consisting of subcapsules which contained the samples. The bend bar samples had at least one side in flush contact with the inside of sub-capsule to allow for heat transfer. Sub-capsules were either 6061 aluminum alloy or V-4Cr-4Ti alloy. The sample temperature was achieved by machining gas gaps into the sub-capsule so that the nuclear heating was conducted through the helium cover gas. A single type-K thermocouple was embedded in each sub-capsule and the temperature was continuously recorded. Following

welding of the aluminum capsule exterior the capsule was evacuated using a turbomolecular pump and back-filled with ultra-high purity helium. This procedure was repeated three times with a final backfill to helium over pressure of 15 psi. The positive pressure of helium was monitored during the irradiation period.

The SiC-1 capsule was inserted into the V-16 in-core thimble of the High Flux Beam Reactor at the Brookhaven National Laboratory. The duration of the irradiation was one reactor cycle which corresponds to an approximate fast neutron fluence of  $1.1 \times 10^{25} \text{ n/m}^2$  ( $E > 0.1 \text{ MeV}$ ). This corresponds to  $\sim 1.1$  displacements per atom (dpa) in SiC, assuming a sublattice-averaged displacement energy of 40 eV. The irradiation temperature for the multilayer-SiC interfacial composite was 385°C and was constant within 5°C throughout the irradiation. Two subcapsules were used for the porous-SiC interfacial composite. The lower temperature subcapsule which was made of type 6061 aluminum alloy had a constant irradiation temperature of 260°C, constant within 5°C throughout the irradiation. The higher temperature subcapsule, which was fabricated from vanadium, initially achieved a temperature of 1060°C and then decreased in temperature linearly with time to a final temperature of 910°C. It is believed that this decrease in temperature is due to swelling of the vanadium subcapsule (associated with interstitial pickup from the capsule gas) which narrowed the gas gap thus reducing the temperature. Other factors such as increased emissivity of the vanadium subcapsule surface would also cause a reduction of the subcapsule temperature. Post-irradiation examination of the SiC samples did not show any evidence of reaction with the subcapsules.

### **Testing**

All transmission electron microscopy was carried out on mechanically thinning and polished samples. For the case of the neutron irradiated specimens, the thickness of the foil was left at greater than 200  $\mu\text{m}$  to minimize grinding damage to the supposed weakened interface. Argon ion milling of was carried out at 15° and 6 keV. All bend testing was conducted at room temperature using a four-point bend fixture with load and support spans of 0.5 and 2.0 cm, respectively. The cross-head displacement speed was  $8.5 \times 10^{-4} \text{ cm/s}$ . Where possible, a furnace anneal at temperature and atmosphere comparable to the in-reactor tests were performed to ensure oxidation or other factors were not responsible for any composite degradation.

## **RESULTS AND DISCUSSION**

Results from the room temperature bend testing for both non-irradiated and 1.1 dpa irradiated composites are given in Table 1. It is noted that data of irradiated bend bars are from two samples at each condition, thus are statistically limited. However, several samples of each type were tested in the non-irradiated condition yielding more statistically meaningful data. The matrix micro cracking stress was taken from the load-displacement curve as the departure from linearity and is therefore a macroscopic matrix stress. Undoubtedly, limited matrix micro cracking occurs at stresses below this value. From the table it is seen that the results from the furnace anneal of control samples was within statistical scatter of the non-annealed control samples. Though it is noted that the ultimate fracture stress for the multilayer SiC interphase appears low.

From Table 1, within statistical limitations, the macroscopic matrix microcracking stress is unchanged. The ultimate fracture stress appears to be reduced in each case, with the multilayer SiC interphase showing the least reduction ( $\sim 8\text{-}20\%$ ) and the porous SiC interphase showing the most ( $\sim 35\%$ ).

Interphase Type	Matrix Microcracking Stress (MPa)	Ultimate Fracture Stress (MPa)
Multilayer SiC		
Non-irradiated	250±32 (6 tests)	507±75
Non-irradiated, 385°C anneal	264±17 (5 tests)	438±21
Irradiated, 385°C	290, 244	462, 371
Pyrolytic Carbon		
Non-irradiated	214±38 (4 tests)	375±51
Irradiated, 385°C	172, 285	235, 347
Porous SiC		
Non-irradiated	298±22 (8 tests)	515±19
Non-irradiated, 260°C anneal	335, 332	507, 510
Irradiated, 260°C	268, 251	347, 344
Non-irradiated, 1000°C anneal	287, 415	457, 507
Irradiated, 1042→910°C	210, 201	332, 304

Table 1 : Bend Test Results for Hi-Nicalon™/CVI SiC Composites

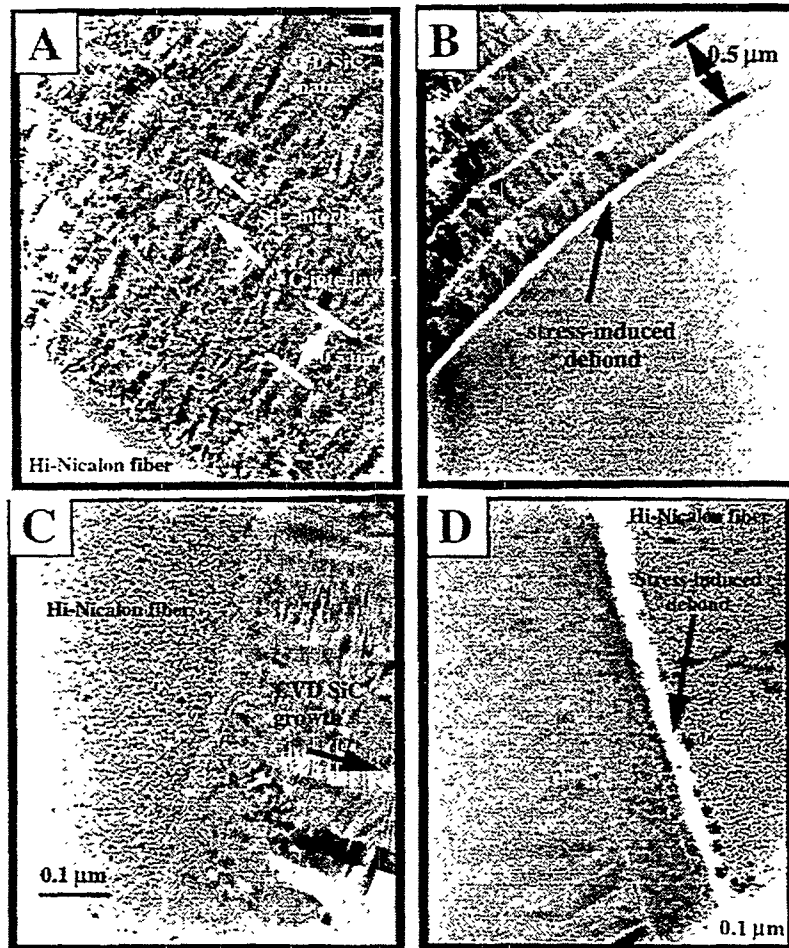


Figure 5: TEM of non-irradiated and irradiated multilayer and porous SiC interphase interfaces.

Transmission electron microscopy reveals debonding at the fiber-interphase boundary for all three interphase materials. For the case of the porous SiC interphase, debonding within the fiber also occurred, though debonding at the boundary was still more common. Non-irradiated (fig 5A,C) and irradiated (fig 5B,D) interphases are shown in Figure 5. A debond width of ~50 nm is clearly visible at the boundary between the fiber and first multilayer (fig 5B). Debonding was observed for regions opaque to the 300 keV electrons indicating that debonding is not due to preferential milling by the argon ions. The micrograph depicting debonding for the porous SiC interphase (fig 5D) is one which exhibited debonding within the fiber. Debond width in this case is on the order of 80 nm. Debonding for the pyrolytic carbon interphase (not shown) occurs at the interface between the fiber and the carbon interphase.

Assuming unirradiated physical properties for fiber and matrix and the irradiation-induced volumetric changes for Hi-Nicalon™ and CVD SiC given in figure 1, a residual stress analysis for the fiber/matrix interface can be performed. The micromechanical analysis of the infiltrated bundle can be simplified by considering a system of three concentric cylinders of increasing radii,  $a$  and  $b$ , where the inner cylinder represents a fiber that is coated by a thin layer of thickness  $(b-a)$ . This bundle is embedded in a matrix represented by a cylinder of radius  $c$  of thickness  $(c-b)$ . The magnitude of  $c$  is selected so that  $v_f = a^2/c^2$ , where  $v_f$  is the fiber volume fraction in the composite. The values of  $a$  and  $b$  are selected from actual values of the fiber radius and the thickness of the fiber coating. To further simplify the analysis, the following assumptions are made: (1) all the phases in the composite are linear elastic and isotropic, (2) no relaxation of stresses during irradiation or during cooling from the fabrication temperature, and (3) fibers and matrix exhibit volumetric changes as a result of neutron irradiation.

Equilibrium of forces in a long cylindrical differential element result in  $\sigma_r = \frac{d}{dr}(r\sigma_\theta)$  and  $\sigma_\theta = \frac{d}{dr}(r\sigma_r)$  where  $\sigma_r$  and  $\sigma_\theta$  are the radial and tangential stresses, respectively and  $r$  is the radial position. When combined, these equations yield solutions of the form:  $\sigma_r = A - \frac{B}{r^2}$  and  $\sigma_\theta = A + \frac{B}{r^2}$  where  $A$  and  $B$  are integration constants that have different values for each of the three phases in the model composite. Boundary conditions require continuity of traction at the fiber-fiber interphase, and at the fiber-interphase-matrix interfaces and zero-normal forces acting on the free surface, i. e.:  $\sigma_r^f(r=a) = \sigma_r^c(r=a)$  ,  $\sigma_r^c(r=b) = \sigma_r^m(r=b)$  , and  $\sigma_r^m(r=c) = 0$ . Upon enforcement of the boundary conditions, the unknown integration constants  $A$  and  $B$  can be eliminated in favor of the still unknown interfacial normal stresses,  $P_1$  and  $P_2$  as follows

$$\sigma_r^f = \sigma_\theta^f = -P_1 \quad r \leq a \quad (1)$$

$$\sigma_r^c = \frac{P_1 a^2 - P_2 b^2}{b^2 - a^2} + \frac{a^2 b^2 (P_2 - P_1)}{r^2 (b^2 - a^2)} \quad a \leq r \leq b \quad (2)$$

$$\sigma_\theta^c = \frac{P_1 a^2 - P_2 b^2}{b^2 - a^2} - \frac{a^2 b^2 (P_2 - P_1)}{r^2 (b^2 - a^2)} \quad a \leq r \leq b \quad (3)$$

$$\sigma_r^m = \frac{P_2 c^2}{c^2 - b^2} \left( 1 - \frac{c^2}{r^2} \right) \quad b \leq r \leq c \quad (4)$$

$$\sigma_\theta^m = \frac{P_2 c^2}{c^2 - b^2} \left( 1 + \frac{c^2}{r^2} \right) \quad b \leq r \leq c \quad (5)$$

Deformation compatibility requires that the radial displacement (e.g., the tangential strains) be the same at the interface for the phases meeting there. Mathematically this is expressed as:  $\varepsilon_\theta^f = \varepsilon_\theta^c, r = a$  and  $\varepsilon_\theta^c = \varepsilon_\theta^m, r = b$ . By assuming a long cylindrical assembly, end-effects are neglected and mathematically the plane-strain assumption is expressed as:  $\varepsilon_z^f = \varepsilon_z^c = \varepsilon_z^m$ , which means that plane cross-sections will remain plane after deformation.

Equilibrium of axial forces requires that the sum of forces in the z direction be equal to zero, i.e.,

$$\frac{a^2}{c^2} \sigma_z^f + \frac{(b^2 - a^2)}{c^2} \sigma_z^c + \frac{(c^2 - b^2)}{c^2} \sigma_z^m = 0 \quad (6)$$

Because the phases are assumed to be both isotropic and perfectly elastic, the relationship between the stresses and the strains will be given by:

$$\varepsilon_r = \frac{\sigma_r}{E} - \frac{\nu}{E} (\sigma_r + \sigma_\theta + \sigma_z) + \alpha \Delta T + \varepsilon_r^o \quad (7)$$

$$\varepsilon_\theta = \frac{\sigma_\theta}{E} - \frac{\nu}{E} (\sigma_r + \sigma_\theta + \sigma_z) + \alpha \Delta T + \varepsilon_\theta^o \quad (8)$$

$$\varepsilon_z = \frac{\sigma_z}{E} - \frac{\nu}{E} (\sigma_r + \sigma_\theta + \sigma_z) + \alpha \Delta T + \varepsilon_z^o \quad (9)$$

where  $\alpha$  is the linear coefficient of thermal expansion,  $\Delta T$  is the change in temperature from the fabrication temperature to room temperature and  $\varepsilon^o$  is the transformation strain resulting from neutron irradiation. Substituting the expression for the stresses (Equations 1-5) into the constitutive equations (Equations 7-9) and enforcing the boundary conditions in Equations (6-8) yields a  $4 \times 4$  system of linear simultaneous equations for the unknown interfacial pressures  $P_1, P_2$  and the axial stresses in the fiber and the fiber coating. The axial stress in the matrix can then be readily determined from Equation 6.

Figure 6 shows the predicted radial stress at the fiber-fiber coating interface as a function of neutron irradiation. Note that those stresses would exist if there continuity of radial displacement existed at the interface. At the 1.1 dpa dose level of this study figure 6 yields a residual stress above one GPa, which is clearly higher than could be withstood by the interphases leading to debonding.

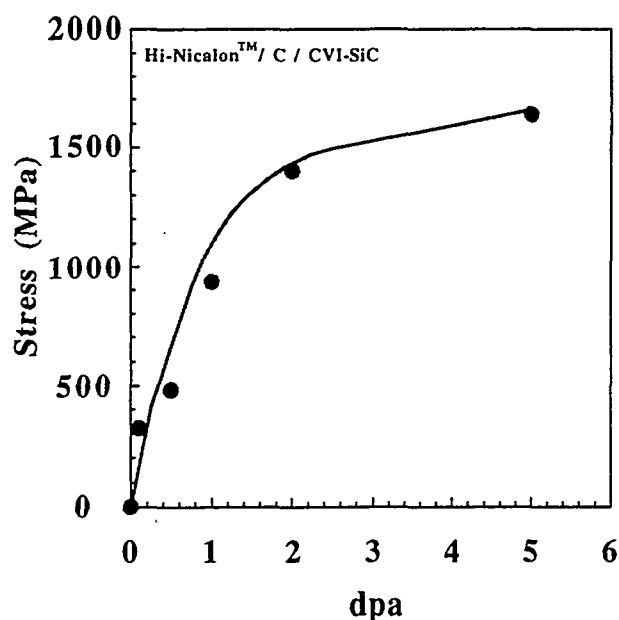


Figure 6: Residual stress at interphase.

## CONCLUSIONS

- (1) Bend strength results indicate that at 1.1 dpa ultimate fracture strength is decreased for Hi-Nicalon™ composites. The relative degree of decrease appears to depend on the interphase type with multilayer SiC interphase suffering the least reduction (~8-20%), followed by the pyrolytic carbon interface (~22%) and the porous SiC interphase (~35%).
- (2) Transmission electron microscopy reveals debonding at or near the interface between the fiber and interphase.
- (3) Residual stress analysis indicates that radial tensile stresses develop at the interphase during irradiation due to induced densification of the Hi-Nicalon™ fiber. These stresses are considerably higher than can be withstood by these or any viable SiC/SiC interphase, indicating that high Nicalon™ is of limited application in neutron irradiation environments.

## REFERENCES

- [1] K. Okamura, A. Matasuzawa, and M. Sato, *J. Nucl. Mater.* 155-157 (1985) 329.
- [2] A. Kohyama, H. Tezuka, and S. Saito, *J. Nucl. Mater.* 155-157 (1988) 334.
- [3] L.L. Snead, M. Osborne, and K.L. More, *J. Mater. Res.* 10 (1995) 736.
- [4] L.L. Snead, D. Steiner, and S.J. Zinkle, *J. Nucl. Mat.* 191-194 (1992) 566.
- [5] L.L. Snead et al., *J. Nucl. Mater.* 253 (1998) 20.
- [6] T. Seguchi, N. Kasai, and K. Okamura, *Proceedings of International Conference on Evolution in Beam Applications*, 1991) p. .
- [7] R.A. Lowden and K.L. More, in *Interfaces in Composites*, Vol. 170, eds. C.G. Pantano and E.J.H. Chen (MRS, Pittsburgh, 1990) p. 273.
- [8] T.M. Besmann et al., *J. de Physique* 50 (1988) 273.